Brian P. DeJong[1]
School of Engineering and Technology,
Central Michigan University,
Mount Pleasant, MI 48859
e-mail: b.dejong@cmich.edu

J. Edward Colgate
e-mail: colgate@northwestern.edu

Michael A. Peshkin
e-mail: peshkin@northwestern.edu

Department of Mechanical Engineering,
Northwestern University,
Evanston, IL 60208

A Cyclic Robot for Lower Limb Exercise

This paper presents the design and simulation of a cyclic robot for lower-limb exercise robots. The robot is designed specifically for cyclic motions and the high power nature of lower-limb interaction—as such, it breaks from traditional robotics wisdom by intentionally traveling through singularities and incorporating large inertia. Such attributes lead to explicit design considerations. Results from a simulation show that the specific design requires only a reasonably sized damper and motor. [DOI: 10.1115/1.4004648]

1 Introduction

A growing number of today's robots are meant for physical interaction with humans. Humanoid robots shake hands and dual-manipulate objects, haptic robots simulate textures and environments, medical robots improve diagnostics and surgery, and assistive robots aide accessibility and rehabilitation.

However, only a small subset of these robots are designed for *lower-limb* interaction, although the need exists. In the exercise realm, such robots can provide full customization of foot pedal paths and dynamics, giving users a flexibility that current exercise machines do not offer. In rehabilitation, these robots can improve patients' recoveries, allowing for targeted, asymmetrical exercise routines. In psychophysiology, lower-limb robots can help researchers find ways to reduce the perceived exertion within exercise, whether through changes in the kinematics or dynamics, or through haptic cues at the pedals. And in physiology, these robots can support the study of the human body and how it works. These are all applications of *haptic lower-limb exercise robots.*

Lower-limb interaction is a particularly difficult aspect of physical human-robot interaction. Conventional design and control methods are not directly extendable to lower-limb exercise as discussed below. Figure 1 shows a graphic that distinguishes lower-limb exercise robots from existing devices.

For example, lower limb activity typically involves cyclic motions, such as walking, running, stair climbing, and skiing. There are many traditional mechanisms designed specifically for cyclic motions, but not so in robotics. Furthermore, almost all machines designed for (noncircular) cyclic motion involve linkages that travel repeatedly through singularities; traditional robotics emphatically avoids singularities because of the resulting degradation of controller performance. Can lower-limb robots be designed such that they repeatedly, intentionally, and successfully travel through singularities?

Second, lower-limb interaction involves large forces and powers to and from the user. Conventional haptic devices cannot handle such interaction, yet lower limb exercise machines can. Most lower-limb robots achieve large forces via large motors that are power consuming and potentially less safe than passive elements. What can be done to minimize motor size? How can the devices be designed to be strong, yet as safe as a motor-less exercise machine?

Finally, users often desire assistance in exercise machines to help carry them around the pedals' paths. Exercise machines use inertia to do so. Traditional robotics wisdom, however, says to minimize inertia so that actuators do not need to overcome it—a problem that (one-degree-of-freedom) exercise machines do not have. Can inertia be incorporated into an (multidegree-of-freedom) exercise robot? Can it be added such that the path actuators do not have to fight it?

This paper attempts to answer these questions by presenting a solution. Here, we discuss a novel design for a lower-limb haptic exercise robot that successfully provides cyclic motion while handling large forces, large powers, and high inertias, all with the potential to be energetically passive. The following sections include background, characteristics of lower-limb exercise robots, resulting design considerations, our specific design, and results from a simulation.

2 Background

2.1 Motivation. Motivation for this device was born from a desire for an all-in-one lower-limb cardiovascular exercise machine [1]. Such a device can allow full customization of the pedal path and dynamics. Users (or trainers) can modify a path shape to their preferences, customize how much the device carries them (inertia), how difficult it is to move the device (damping), and fluctuate these properties within a pedal cycle or workout. Furthermore, an all-in-one robot can simulate the existing ellipticals, stair climbers, ski machines, bicycles, treadmills, and arc trainers—users do not need to switch machines to vary their workout.

A lower-limb haptic robot also has application in the rehabilitation field. Studies show that aerobic exercise during stroke rehabilitation improves strength and motor control of lower extremities, as well as aerobic and cardiovascular conditioning (e.g., Ref. [2]).

Recovering patients with high-functioning lower limbs can use lower-limb haptic robots for general exercise, but more importantly, for exercise that is customizable to their specific, even anisotropic or asymmetrical, needs. A haptic robot could provide the desired path with or without assistance, and with the desired resistance. It can interact with only one leg, both legs independently, or both legs dependently. Furthermore, it can isolate specific muscles for more efficient rehabilitation [3].

Motivation for lower-limb haptic robots also comes from the psychophysical research field. Of significant interest is a study done by Zeni et al. [4]. Zeni and his colleagues tested users on various types of cardiovascular exercise machines (including stair climbers, treadmills, and bicycles), and found that, for the same level of power output, some machines felt more exhausting than others [4]. The results from an experiment run by Glass and Chvala support these findings [5]. A preliminary experiment by DeJong et al. found that increasing a device's inertia may decrease

[1]Corresponding author.

Manuscript received July 19, 2010; final manuscript received June 7, 2011; published online August 15, 2011. Assoc. Editor: Just L. Herder.

 Copyright © 2011 by ASME

Downloaded 25 Aug 2011 to 141.209.167.245. Redistribution subject to ASME license or copyright; see http://www.asme.org/terms/Terms_Use.cfm

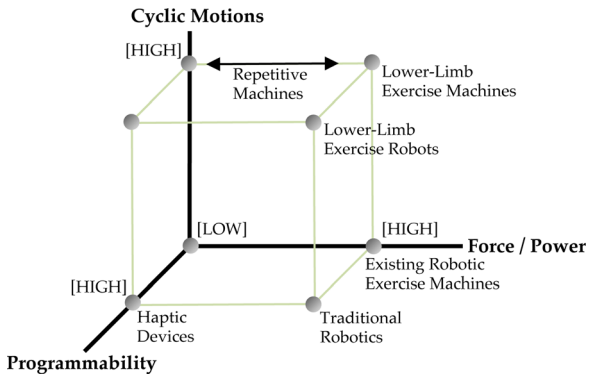

Fig. 1 Comparison between lower-limb exercise robots and other devices

the perceived level of workout by the user [6]. These studies, along with plenty of anecdotal evidence, suggest that exercise machines and robots can be designed to optimize users' workouts while reducing the perceived exertion.

Also within the psychophysical field is research into applying control and cuing techniques to help users maintain a certain level of exercise speed or intensity. Horowitz et al. applied an adaptive damping controller to a modified stair climber to maintain users' step rates [7]. Similarly, Ferber ran human experiments on another robotic stair climber, testing haptic cuing at the pedals [8].

Another area of motivation for lower-limb haptic exercise robots is physiological research: an exercise robot that can isolate a trajectory or muscle group in a leg can be used to study the human body and how it works.

Finally, motivation comes from the robotics research field itself. Traditional robotics wisdom says to minimize inertia and avoid singularities—can robots be designed that successfully break these guidelines?

2.2 Existing Devices. There are many existing devices meant for lower-limb interaction, although most have limited programmability. In the last two decades, the consumer exercise market has seen significant growth in the array of lower-limb cardiovascular machines, with machines such as bicycles, treadmills, stair climbers, ski machines, arc machines, and ellipticals. These machines offer user-selectable damping levels usually achieved by an electronically controlled alternator [8].

Elliptical exercise machines are named for the roughly elliptical shape of their pedal paths, although the exact path is not truly elliptical. Ellipticals have a damped flywheel attached to the pedals via a linkage. Several designs include secondary linkages that stretch or deform the shape of the pedal path from that of the simpler four-bar versions. Path shapes depend on the device's mechanism with no two brands alike. In fact, many of the path shapes are far from elliptical. Actual path shapes range from warped and bent loops to teardrop shaped [6].

Ellipticals have recently begun to incorporate limited programmability in their path shapes. Most of this flexibility affects the stride length, although examples exist of programmable tilt of the path/mechanism or compliant components for the ankle angle.

A few consumer stair climbers have be refitted with motors for reprogrammability (e.g., Refs. [7, 8]). However, these devices still have one-dimensional pedal paths.

In rehabilitation, there are several commercially available robots for gait rehabilitation that incorporate footpaths. For example, the Lokomat [9] and the LOPES [10] use exoskeletons, while the Gait Trainer [11] and the Haptic Walker [12] use foot pedals. Rehabilitation still relies heavily on simple devices like bicycles and treadmills.

For use with virtual reality, several locomotion devices have been built. These devices employ pedaling (e.g., Ref. [13]), programmable foot platforms (e.g., Ref. [14]), or treadmills (e.g., Ref. [15]).

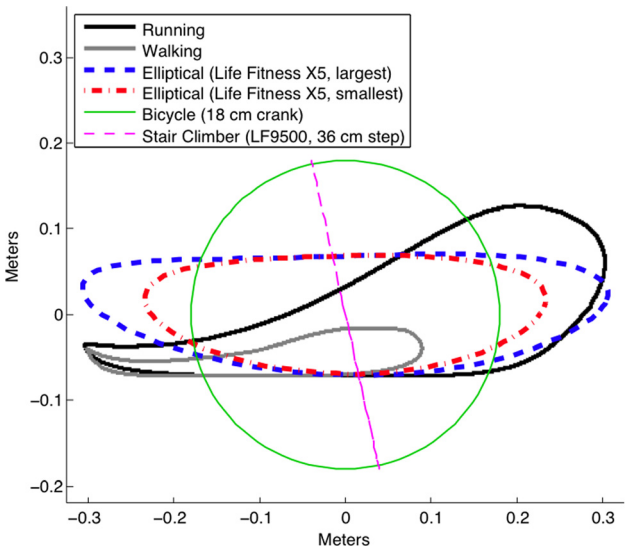

Fig. 2 Sample foot paths for exercise (user is facing to the left). Running and walking paths were obtained by analyzing video available from Ref. [22] and by modifying a figure in Ref. [23]; other paths are as modeled.

Finally, a few robotic devices have been designed to simulate free weights using motors or brakes (e.g., Ref. [16]). None of these robots received further investigation after being built.

3 Class Characteristics

Let us now look at some characteristics of lower-limb haptic exercise robots (see also Ref. [1]).

3.1 Programmability. Lower-limb exercise robots should allow users to fully customize, i.e., program, the device. Current exercise machines offer basic programmability, such as the damping level and more recently the stride length. Yet much more programmability is desired: from tweaks of the path shape to tuning of the path dynamics.

3.2 High Quality Constraints. For lower-limb exercise, robots must impart constraints on the user's motion, guiding the pedals along the path. In most cases, these constraints should be stiff and smooth—stiff perpendicular to the path, yet smooth tangent to it.

3.3 Cyclic Motions. The first major distinction between robots for lower-limb exercise and other haptic applications is the cyclic nature of the pedal paths. Unlike upper-body motion, most lower-limb motion is cyclic. Existing exercise machines offer a variety of cyclic pedal paths—see Fig. 2 for a comparison of foot paths. An average workspace is under 55 cm fore-aft (for ellipticals, maximum is around 80 cm) and 36 cm vertically (for stair climbers, maximum is around 55 cm) [6].

3.4 High User Force. Another result of interaction with lower-limbs is that the exercise device must be able to impart high forces. Users are able to push down on the pedals with forces greater than their weight, and the robot must withstand these forces to keep the pedal on its path.

To understand the forces involved in cardiovascular exercise, we fitted a Life Fitness X5 elliptical with a force sensor under one pedal and measured forces during various workloads. The pedal

Downloaded 25 Aug 2011 to 141.209.167.245. Redistribution subject to ASME license or copyright; see http://www.asme.org/terms/Terms_Use.cfm

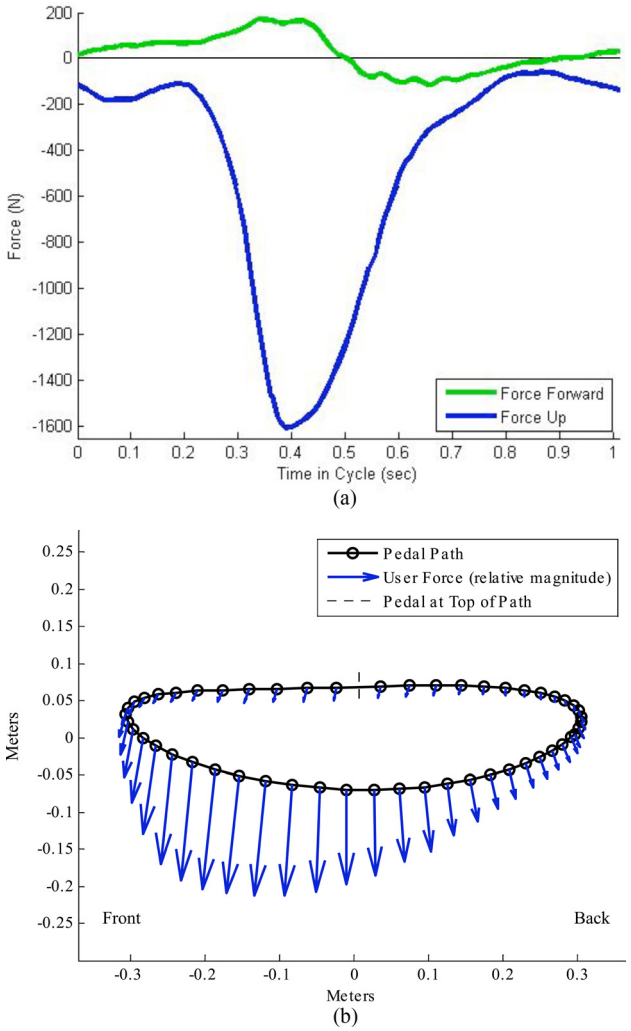

Fig. 3 User forces measured on Life Fitness X5, for a 104 kg user, during normal operation, at approximately 60 rpm. User is facing to the left. (*a*) Forces versus time (*b*) Force direction within one cycle (path as modeled).

cycle with the highest resulting force is shown in Fig. 3. These results are from a relatively normal style of operation by a 104 kg user. Vertical forces peaked around 1600 N (1.6 body weights), and fore-aft forces reached just under 200 N (0.20 body weights). Examination of directionality (Fig. 3(*b*)) shows that the maximum force occurred in the lower front of the stride, i.e., when the user was shifting his weight onto his forward foot.

3.5 High User Power. Lower-limb haptic exercise robots also encounter high instantaneous power *to* and *from* the user. It is well known that humans can output many hundreds of watts of mechanical power during peak exertion loads. Even moderate exercise involves several hundred watts: the U.S. Department of Health and Human Services defines moderate exercise as exertion of around 250–500 watts [17]. Researchers [4,18–20] have measured average "moderate"[2] power outputs anywhere from 250 to 650 watts.

Conversely, during some parts of lower-limb exercise, there may be many watts of power from the device *to* the user. If users are imperfect in their exercise—and they most certainly are—then they can be expected to do negative work on the exercise device, such as temporarily riding an elliptical's pedal. This negative power is on the order of hundreds of watts: e.g., lifting the user's mass (e.g., 100 kg) at a typical speed (e.g., 1.0 m/s).

3.6 User Workout. Not only is the user imparting high instantaneous power to the exercise device, and *vice versa*, but also the net power is large and into the device. That is, users are putting much net energy into the machine or robot, because they want a workout. Typical average numbers for cardiovascular exercise are on the order of several hundred watts (previous section). Lower-limb haptic exercise robots need to be able to receive this amount of energy, and they should do something intelligent with it, such as shuffle it around and reuse it, rather than simply burning it off as heat.

3.7 Large Inertia. Unlike traditional robots, lower-limb exercise robots should assist the user through parts of the cyclic path. Most cardiovascular exercise machines used highly geared flywheels to do this. For example, the previously measured Life Fitness elliptical has a flywheel geared at a measured 9.33 to 1. The flywheel has an effective inertia of around 10.6 kg m^2 [6]. At 60-rpm pedal speed, it is storing around 200 J.

3.8 Low Power Consumption. As with all haptic devices, lower-limb exercise robots should be designed to minimize power consumption. This involves using the smallest motors possible as well as reusing the energy received from the user. Ideally, the devices will require no additional power from a wall outlet—in fact, many existing bicycles, stair climbers, ski machines, and passive treadmills achieve this.

3.9 Safety. The most important attribute of haptic lower-limb exercise robots is that of user safety. While this is an obvious concern in the design of any device that interacts with a human, safety means that scaling existing active, haptic robots is not desired, as the resulting large motors are potentially unsafe for interaction with the user. Therefore, exercise robots should be as passive as possible, with several layers of safety checks implemented. Ideally, the robot would be more safe than the existing passive exercise machines.

These nine attributes help characterize lower-limb haptic exercise robots. But how do these robots compare to existing devices? What are the existing devices' limitations?

Table 1 compares lower-limb exercise robots to existing commercial exercise machines, robotically modified exercise machines, and haptic devices. Clearly, these existing devices cannot be extended to lower-limb haptic exercise.

4 Design Considerations

Let us look at how these class characteristics influence the design of lower-limb exercise robots. A good way to approach the design is to separate the requirements of the device perpendicular

Table 1 Comparison of attributes between lower-limb exercise robots and existing devices

	Lower-Limb Exercise Robots	Consumer Exercise Machines	Robotically Modified Exercise Machines	Haptic Devices
Program.	High	Low	Low	High
Constr. Qual.	High	High	High	High
Motions	Cyclic	Cyclic	Various	Various
User Force	High	High	High	Low
User Power	High	High	High	Low
User Workout	High	High	High	Low
Energy Stor.	High	High	Low	Low
Power Use	Low	Low	Low	Low
Safety	High	High	High	High

[2]As defined by the corresponding authors.

Downloaded 25 Aug 2011 to 141.209.167.245. Redistribution subject to ASME license or copyright; see http://www.asme.org/terms/Terms_Use.cfm

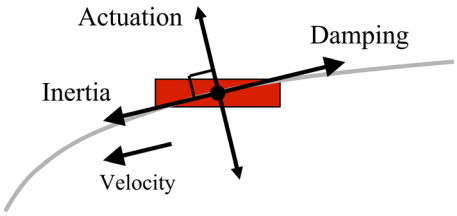

Fig. 4 Foot pedal on the sample path. The arrows show separation of path actuation (perpendicular) from inertial and damping forces (parallel).

versus parallel to the path. Figure 4 shows a sketch of a pedal on a sample path. The device must constrain the pedal (and thus the user) *to* the path, and impart inertia and damping *along* the path. This is similar to steering versus propulsion.

4.1 Actuators and Passivity. The perpendicular path constraint should be of high quality: stiff and smooth. Such constraints can be easily achieved if the device's linkage is locked into a one-degree-of-freedom mechanism. Although the device may have a set of attainable pedal paths that exist in a multidimensional workspace, each individual path requires one degree of freedom. If the device's actuators are locked such that the resulting one-degree-of-freedom mechanism achieves the desired path, that path will be stiff and smooth.

Realistically, one or more actuators may need to be moving to achieve the desired path. These actuators should move the pedal perpendicular to the path, and not parallel to it. If the actuators do not affect the position of the pedal along the path, then the actuators do not have to simulate or overcome the path's inertia or damping.

What is important is that the robot conceivably could be passive, even with imperfect efficiencies of its components. Because the user is putting significant net energy into the device (it is exercise, after all), the device should be receiving enough extra energy to overcome its loses. An ideal device would be able to store energy and return it, without requiring more energy than what the user has already given it.

4.2 Inertia and Damping. Meanwhile, the motion parallel to the path should have large inertia and damping. This inertia and damping should affect the parallel motion *only*; perpendicular will interfere with any path-constraint actuators. When constrained to parallel motion only, the damping is always removing energy and can be achieved by a passive element.

4.3 Singularities. Robotics and cyclic motions devices differ with regard to singularities. Traditional robotics wisdom says to avoid singularities at all costs because the path controller behaves poorly near them. But singularities are common in machines that generate repetitive motion; often inertia carries the device through them.

As in traditional robotics, the singularities in lower-limb exercise result in a loss of mobility, as higher-dimensional workspaces flatten at singularities. With regard to users, the loss of mobility may actually help maintain high quality constraints—users' inputs have less effect perpendicular to the path near the singularities. Users' influences tangent to the path will also decrease, which means they cannot as easily speed up or slow down the mechanism.

The singularities may cause problems for the controller, but there are solutions. For example, the controller could soften (or even turn off) near singularities to maintain stability (since the user's influence is less). Or the path and controller could be transformed to a workspace without singularities; if the path and controller are across a singularity from the user, then stable control is even easier.

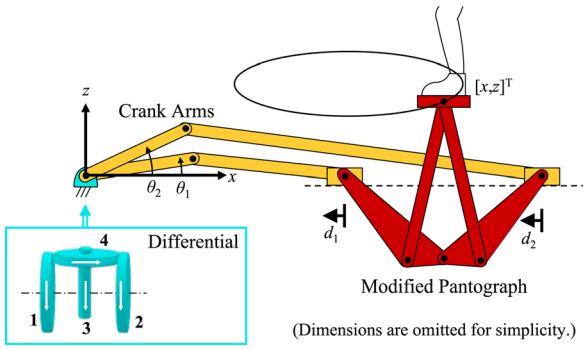

Fig. 5 The specific design, colored for the three subsystems

Therefore, with inertia and an intelligently designed controller, lower-limb exercise robots should be able to travel through singularities.

5 A Specific Design

We now present a specific design for a lower-limb haptic exercise robot that successfully travels through singularities and incorporates inertia. While the design may seem complex at first, the reasoning for each component is well founded.

The design focuses on only one leg, i.e., one side, of the device. This is to simplify the problem but also because the second leg can be identical to the first and coupled through a mechanism such as that discussed in Ref. [6].

In all of the figures, the user is facing to the left, although it is not drawn to scale.

5.1 Overview. The design is shown in Fig. 5. On the upper-right is a pedal that travels in a path, such as the ellipse drawn. The mechanism consists of three subsystems: the pedal-supporting Modified Pantograph, the cyclic-motion-creating Crank Arms, and the phase-isolating Differential.

The pedal is supported by the Modified Pantograph subsystem. The pedal's position, $[x,z]^T$, is related to the linear positions of the two sliders: d_1 and d_2. These sliders are constrained to the horizontal axis, such as by linear rails. By moving the sliders in unison, the device moves the pedal in the x direction, and by moving the sliders in equal and opposite directions, the device moves the pedal in the z direction.

The Modified Pantograph design is complex, but it evolved from a much simpler design. It is optimized for stability and efficiency. See Ref. [6] for more details.

The second subsystem is the Crank Arms. Since the pedal is to travel in cyclic paths, the sliders need to travel forward and backward along their rails, and this is accomplished by two rotating crank arms. As we will show in Sec. 5.2, the two crank arms rotate in near unison.

The design is functional with just the Crank Arms and Modified Pantograph; however, it has one major drawback. Suppose the mechanism is at the configuration shown in Fig. 5.[3] The major component of a user's force is downward—such a force creates equal and opposite forces on the sliders, trying to pull them together. These forces are transmitted to the crank arms, resulting in torques trying to pull the crank arms apart. This means that any actuators on θ_1 and θ_2 must exert opposite (and large) torques to guide the pedal. Since the crank arms are almost always on the same side of the horizontal axis, *the opposite torques are almost always occurring*.

Adding the Differential subsystem improves the design. A differential consists of four main parts—the differential in Fig. 5 is

[3]This problems holds for any configuration where the two crank arms are on the same side of the horizontal axis.

Downloaded 25 Aug 2011 to 141.209.167.245. Redistribution subject to ASME license or copyright; see http://www.asme.org/terms/Terms_Use.cfm

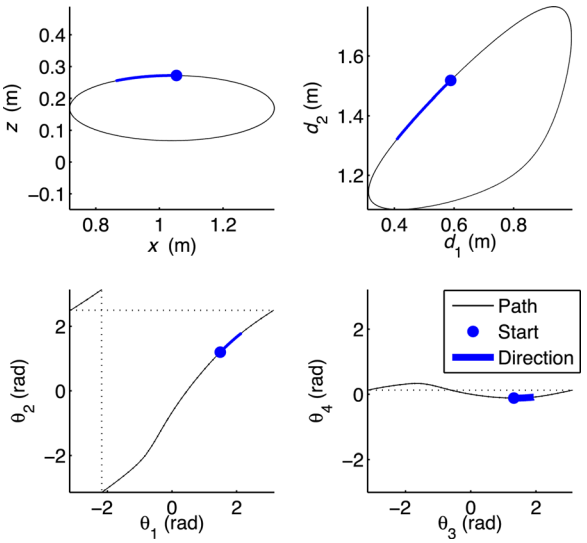

Fig. 6 The sample pedal path in the four spaces

drawn with friction contacts although it could use gears instead. Two wheels (or gears), labeled 1 and 2, and a shaft, labeled 3, rotate about a common axis. Each wheel is in contact with a third wheel, labeled 4, which rotates about shaft 3. Shaft 3 does not rotate about its length. For this paper, we assume that 1, 2, and 4 have the same radii.

The Differential's angular velocities ($\theta's$) and torques ($\tau's$) are related as

$$\begin{bmatrix} \dot{\theta}_3 \\ \dot{\theta}_4 \end{bmatrix} = \begin{bmatrix} \frac{1}{2} & \frac{1}{2} \\ \frac{1}{2} & -\frac{1}{2} \end{bmatrix} \begin{bmatrix} \dot{\theta}_1 \\ \dot{\theta}_2 \end{bmatrix} \tag{1}$$

$$\begin{bmatrix} \tau_3 \\ \tau_4 \end{bmatrix} = \begin{bmatrix} 1 & 1 \\ 1 & -1 \end{bmatrix} \begin{bmatrix} \tau_1 \\ \tau_2 \end{bmatrix} \tag{2}$$

Therefore, θ_3 is the average velocity of 1 and 2, while θ_4 is the difference. That is, θ_3 is the average motion of the device around its cyclic path, while θ_4 is the rate of change of the angle between 1 and 2.

Meanwhile, the torque on 3 is the sum of the torques of 1 and 2, while the torque on 4 is the difference. This means that for opposite torques on 1 and 2 (as mentioned before), τ_3 is small while τ_4 is large.

The significance of the Differential will become clearer when we discuss the idea of phasing in Sec. 5.2, and from the simulation results in Sec. 6.2. The Differential allows actuation of 3 and 4. Figure 6 shows the pedal path in the four different spaces.

5.2 The Concept of Phase. One of the important ideas in the analysis of this device is the concept of phase. The crank arms are to continuously rotate, driving the pedal around its path in $[x,z]^T$. Suppose the crank arms are aligned (i.e., $\theta_1 = \theta_2$) as shown in Fig. 7(*a*), and rotating at the same speed (i.e., $\theta_1 = \theta_2$). The sliders travel forward and backward, nearly in unison, and thus the pedal travels in an almost horizontal path.[4] Suppose instead that the crank arms are pointing in opposite directions (i.e., $\theta_1 = \theta_2 + \pi$) as shown in Fig. 7(*b*) but still rotating at the same speed. The sliders move in opposite directions, and the pedal travels in a nearly vertical path. Finally, suppose that the angle between the crank arms is neither 0 nor π, as in Fig. 7(*c*). In this case, the pedal travels in a loop in its space.

The angle, i.e., *phase*, between the crank arms is important. The constant-phase paths shown in Fig. 7 are very similar to paths created by existing exercise machines: a ski machine, a stair climber, and an elliptical.

The set of constant-phase paths for the device is shown in Fig. 8(*a*). As the phase increases from 0 to π, the loops gradually open vertically and close horizontally.[5] By changing the phase within a cycle, the device can transition from one loop to another, achieving the desired path (Fig. 8(*b*)). This path requires the phase values shown—the change in phase is relatively small throughout the cycle. The differential helps the design because it isolates this phase via θ_4 (see Ref. [2]). Thus, θ_3 represents the *generic position* around the path, while θ_4 is essentially the *phase*.

5.3 Adding Inertia, Actuation, and Damping. Given the concept of phase and generic motion, where should inertia be incorporated?

The inertia should be added so that it helps carry the user around the path. The logical place for it, therefore, is on θ_3 so that it affects the generic motion around the path. If the dominant inertia in the device is via a flywheel on θ_3, then θ_3 will stay relatively constant within a cycle.[6]

Clearly, constant flywheel speed does not correspond to constant path speed. In fact, the speed along the path varies due to the linkages separating the pedal from the flywheel. This is common in existing exercise machines, and yet it is not unpleasant to the user.

Path actuation ($\boldsymbol{F}_{Path}$) should be added such that it provides a path-restoring force without affecting inertial speed ($\boldsymbol{x}_{Inertia}$)—recall Fig. 4. Assuming the only inertia is on 3, the user-less device will travel on constant (θ_3,θ_4) paths, i.e., $\theta_4 = 0$. In *xy*-space, we want $\boldsymbol{F}_{Path}$ to be perpendicular to $\boldsymbol{x}_{Inertia}$

$$0 = \boldsymbol{F}_{Path}^T \bullet \dot{\boldsymbol{x}}_{Intertia} = \left[\boldsymbol{J}_{Full}^{-T} \bullet \begin{bmatrix} \tau_3 \\ \tau_4 \end{bmatrix} \right]^T \bullet \boldsymbol{J}_{Full} \bullet \begin{bmatrix} \dot{\theta}_3 \\ \dot{\theta}_4 \end{bmatrix} = \begin{bmatrix} \tau_3 & \tau_4 \end{bmatrix} \bullet \begin{bmatrix} \dot{\theta}_3 \\ 0 \end{bmatrix} \tag{3}$$

so we want $\tau_3 = 0$. Therefore, an actuator on 4 provides a path-restoring force, *without* having to overcome the inertia on 3 and *without* affecting the generic velocity, θ_3.

Following the logic in the last section, we want to create damping along the path so that the user has to exert energy to move the device. That is, the damping force should be parallel to the velocity vector in Fig. 4. Therefore, the damping is determined by τ_3. The damper does not see the actuator on 4, or *vice versa*.

5.4 The Effects of Singularities. Interestingly, this device design readily travels through multiple singularities each cycle. Each crank arm encounters two singularities per revolution: when their links are fully folded and fully extended. Singularities are common in machines that generate repetitive motion, but traditional robotics wisdom says to avoid singularities at all costs because the path controller often behaves poorly near singularities.

What are the effects of the singularities on motion and the path controller? Can we design a robot that purposely and successfully travels through singularities?

5.4.1 Path Restrictions. Recall Fig. 8(*a*) showing constant-phase pedal paths. The set of paths has an odd-shaped boundary to it, emphasized in the figure. This boundary is caused by the device's singularities.

Because the Crank Arms rotate in complete revolutions, they must travel through their fully folded and fully extended singularities. Suppose the device is in the configuration shown in Fig. 9(*a*), with $\theta_1 = \pi$, and $\theta_2 \neq 0$, π. In this configuration, slider 1

[4]The path has some vertical motion because the distal Crank Arm links are not the same length.

[5]The flat top boundary of the set is the result of the maximum possible pedal height based on the Modified Pantograph dimensions.

[6]In actuality, it will vary slightly because of the shuffling of energy to and from the links' masses, and to and from the user.

Downloaded 25 Aug 2011 to 141.209.167.245. Redistribution subject to ASME license or copyright; see http://www.asme.org/terms/Terms_Use.cfm

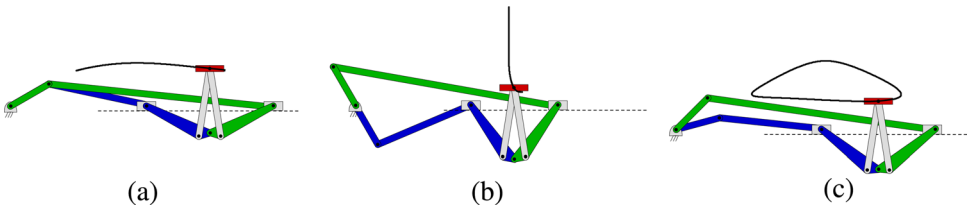

Fig. 7 Sample paths resulting from constant phases (i.e., the angles between the crank arms). (*a*) Phase = 0. (*b*) Phase = π. (*c*) Phase = $\pi/6$.

must be at the given location which means that the pedal must lie on the one-degree-of-freedom arc defined by θ_2. Thus, the two-dimensional pedal space is flattened to a one-dimensional curve, a curve that forms one boundary on the pedal's workspace. Furthermore, the pedal *must* touch (and not cross) this boundary once every cycle.

The second singular configuration for 1 is at $\theta_1 = 0$—see Fig. 9(*b*). Here, 1 is fully extended and the pedal is once again constrained to a one-degree-of-freedom path. As with the other boundary, the pedal must touch this boundary once every cycle for 1 to rotate in complete revolutions.

Similar to 1, 2 has two singularities forming boundaries on the pedal's workspace. In addition, there is a maximum and minimum pedal height defined by the pantograph's geometry, although these boundaries need not be encountered every cycle.

The four singularity boundaries and two height boundaries form the perimeter of the pedal's workspace. All pedal paths *must* touch each of the four singularity boundaries—sample paths that do so are shown in Fig. 10.

The singularities also restrict the set of (monotonically increasing) paths that the device can achieve without further actuation. Paths that do not touch all four boundaries are invalid. However, such paths *can* be achieved by offline actuating the lengths of three of the four Crank Arm links [6].

The path and the device dimensions must be intelligently chosen such that the path touches all four of the singularity boundaries. The process involves an iterative search, because the inverse kinematics are not analytically solvable. See Ref. [6] for a full description of the algorithm. Note that this algorithm is only run when the pedal path is first defined, *not* during operation.

5.4.2 Mobility Issues. As in traditional robotics, the singularities result in a loss of mobility, as the two-dimensional pedal workspace flattens to one dimension at the singularities. The loss of mobility actually helps maintain the path—users' inputs have less effect perpendicular to the path near the singularities. Users' influences tangent to the path also decrease, which means they cannot as easily speed up or slow down the mechanism.

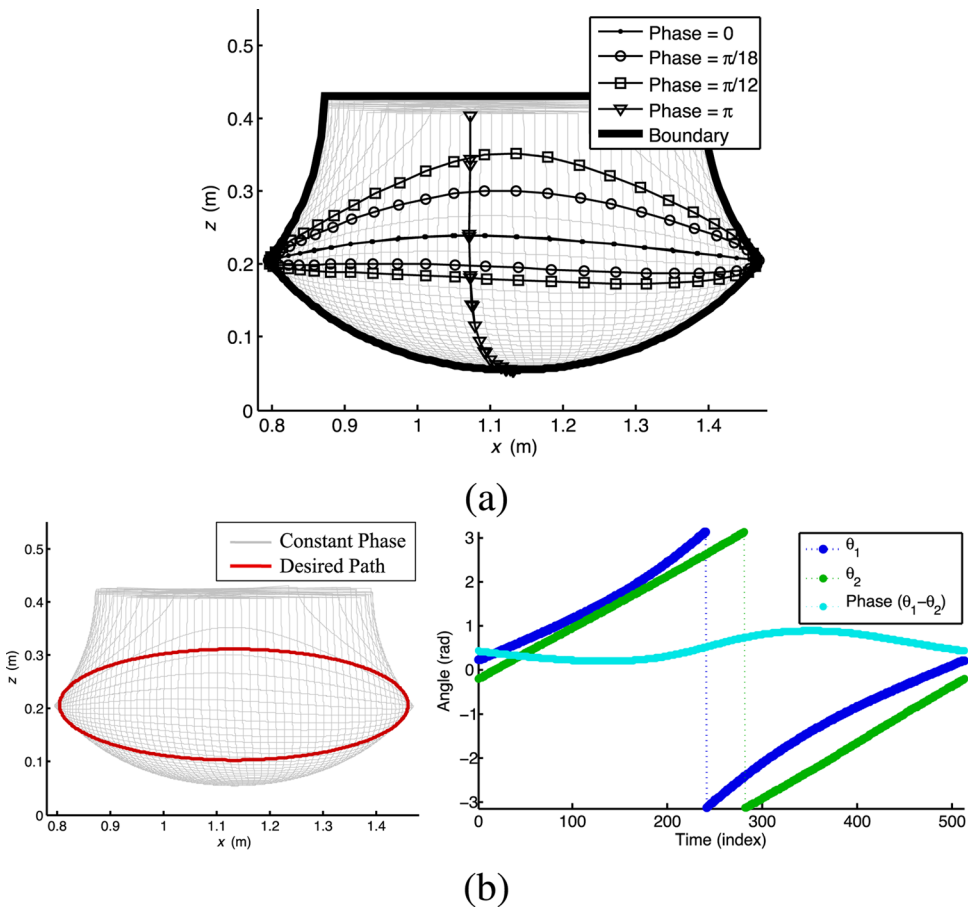

Fig. 8 Phases for paths. (*a*) Set of constant-phase paths. (*b*) One desired path, with resulting phase values.

Downloaded 25 Aug 2011 to 141.209.167.245. Redistribution subject to ASME license or copyright; see http://www.asme.org/terms/Terms_Use.cfm

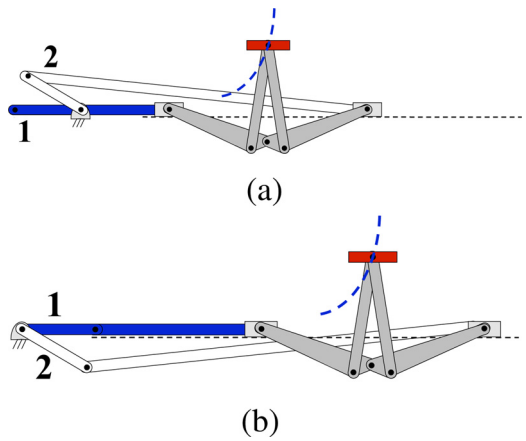

Fig. 9 Path boundary due to singularity at (*a*) $\theta_1 = \pi$, (*b*) $\theta_1 = 0$

Thus, it is important that the device is never at more than one singularity at a time. Graphically, this means the path should never touch the intersection of two singularity boundary curves.

5.4.3 Apparent Inertia. As discussed previously, there is a large inertia attached to 3. Because this inertia is on the opposite side of the crank arms' singularities from the user, the user sees a significant change in the apparent inertia at the pedal as it travels along its path. Yet, such fluctuation is not unpleasant to users, as similar variations exist with existing exercise machines.

To calculate the apparent inertia, m_{App}, we calculate the kinetic energy, assuming the only inertia is on 3:

$$\text{Kinectic Energy} = \frac{1}{2}\dot{\theta}_{34}^T \mathbf{I}_{34}\dot{\theta}_{34} = \frac{1}{2}m_{App}v^2$$
$$m_{App} = \frac{1}{v^2}I_3\dot{\theta}_3^2 \tag{4}$$

where $\mathbf{I}_{34}$ is an inertia matrix, I_3 is the inertia on 3, and v is the tangential velocity of the pedal. Figure 11 shows a plot of m_{App} per unit of mass on I_3, for one cycle. Thus, the user sees from 8 to 136 times the inertia on 3, for an average of around 32 times (equivalent to a 5.7 gear ratio). Further reduction (and thus scaling in inertia) can be accomplished by adding additional gearing to the flywheel on 3.

5.5 Controller Design. In robotics, controllers commonly behave poorly near robots' singularities. This would surely be the case for this device, if the controllers attempted to follow a path in

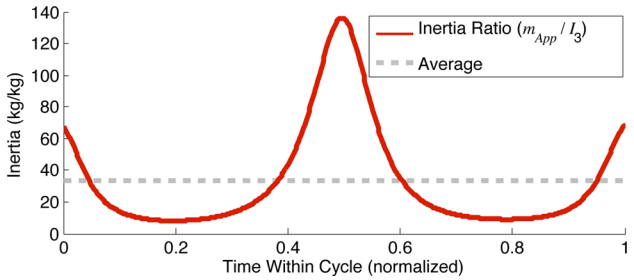

Fig. 11 Apparent inertia (as a ratio of flywheel inertia) along the path

x-space using actuators in $\boldsymbol{\theta}_{34}$-space—if the controller and path are separated by the singularity. As the device approached a singularity, the controller would lose influence, over compensate, and probably cause instability.

However, the issue can be avoided by transforming the desired path into the $\boldsymbol{\theta}_{12}$ or $\boldsymbol{\theta}_{34}$ space. Now the controller does not encounter any singularities in its path, and the pedal successfully follows the desired path in the controller's space.

We further simplify the control by approximating the path as a few-term Fourier summation. Ideally, we would like to define the path analytically, but the dual-valued inverse kinematics of the Crank Arms prevents it. In the $\boldsymbol{\theta}_{34}$-space, the path is close to sinusoidal (Fig. 6), and can be modeled as a three-term Fourier series, with maximum error under a third of a millimeter.

The path controller for the device is similar to ones used in cobotic devices [21]. At each timestep, the controller calculates the position and velocity errors ($\Delta\boldsymbol{\theta}_{34}$ and $\Delta\dot{\boldsymbol{\theta}}_{34}$) based on a reference point (that is tracked by the controller), and calculates a torque based on its gains:

$$\tau_{feedback_{34}} = K \bullet \Delta\theta_{34} + B \bullet \Delta\dot{\theta}_{34} \tag{5}$$

where K and B are gains. The torque is then projected onto the path's current normal to guarantee no effect on motion along the path. The singularities actually help the controller because they reduce the user's influence.

6 Simulation

6.1 Overview. This section presents an in-depth simulation of the device, in MATLAB. The simulation takes into account the masses of the individual links, flywheel inertia and damping torque on 3, a phase actuator torque on 4, and a model of the human's input. Results from the simulation show that this design is a promising lower-limb exercise robot.

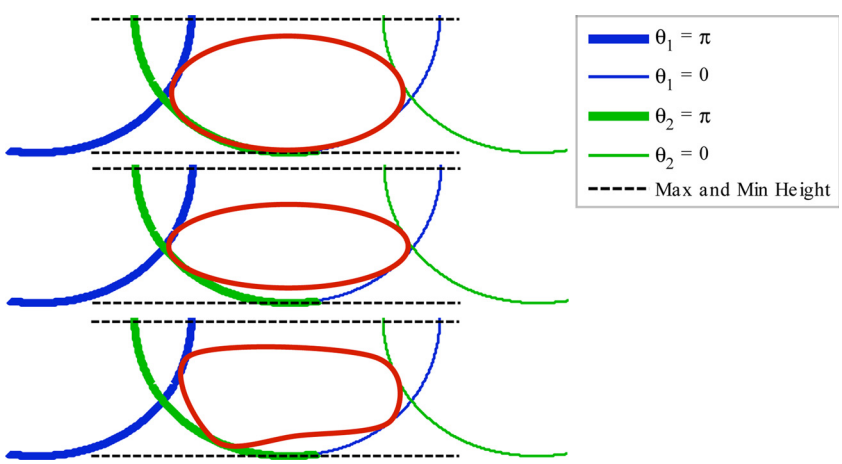

Fig. 10 Sample valid paths that touch all four boundaries

Downloaded 25 Aug 2011 to 141.209.167.245. Redistribution subject to ASME license or copyright; see http://www.asme.org/terms/Terms_Use.cfm

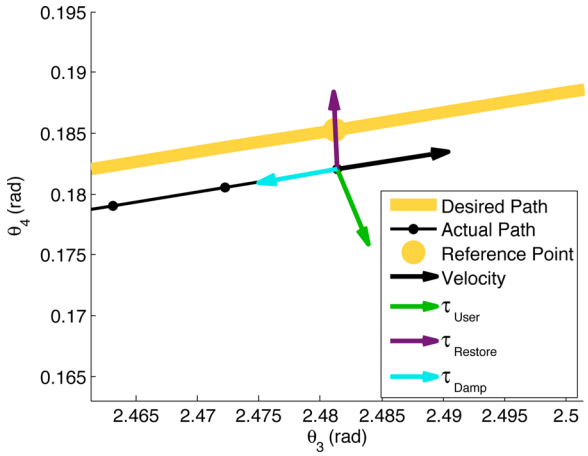

Fig. 12 Torques on the device at the timestep when the user's torque was maximum. Note that at this timestep, τ_{user} is near perpendicular to the path.

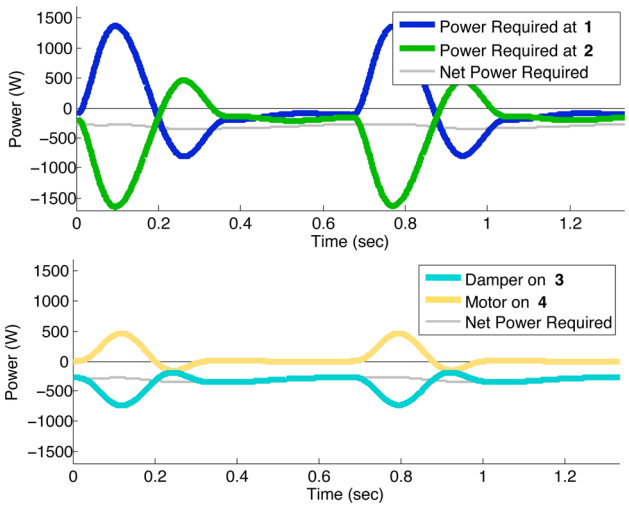

Fig. 13 Power requirements of actuators at 1-2 or 3-4, for two cycles of the path

For the simulation, we defined a rough model of the human's input based on the forces measured on an existing elliptical [6]. For simplicity, we assumed perfectly repetitive users: users push in the same direction at the same part of every cycle. Furthermore, we parameterized the user's force as a function of the generic (monotonically increasing) angle within the cycle. We then parameterize the desired path in terms of the same angle. We transform these points to $\boldsymbol{\theta}_{34}$-space, and thus can plot the user's force versus θ_3. Finally, we approximate the forces as a Fourier Summation, as we did with the path. With 11 terms, the average errors are below 2%.

6.2 Results. The simulation was run for 90-RPM cycles of 300 W user input. The (rotational) inertia and damping were empirically chosen to be 10.0 kg m^2 and 3.5 N m s [6].

The controller in the simulation successfully kept the pedal on the desired path. Maximum position error in the **x** space was less than 2 mm. The controller overcame forces from the user that were almost normal to the path, as can be seen in Fig. 12.

Of significant interest is the power required of the actuators to achieve this path at this damping. From [2], it can be shown that the powers at 1, 2, 3, and 4 are

$$\begin{aligned} P_1 &= \tau_1\dot{\theta}_1 \\ P_2 &= \tau_2\dot{\theta}_2 \\ P_3 &= \tau_3\dot{\theta}_3 = \frac{1}{2}\left(\tau_1\dot{\theta}_1 + \tau_1\dot{\theta}_2 + \tau_2\dot{\theta}_1 + \tau_2\dot{\theta}_2\right) \\ P_4 &= \tau_4\dot{\theta}_4 \end{aligned} \tag{6}$$

Since the design needs little phase change (i.e., θ_4 is small, so $\theta_1 \approx \theta_2 = \theta$), the powers become

$$\begin{aligned} P_1 &\approx \tau_1\dot{\theta} \quad & P_2 &\approx \tau_2\dot{\theta} \\ P_3 &\approx (\tau_1 + \tau_2)\dot{\theta} \quad & P_4 &\approx \tau_4\dot{\theta}_4 \end{aligned} \tag{7}$$

Furthermore, as discussed previously, a vertical force on the pedal (the major direction of the user's input) creates forces in opposite directions on the sliders, and thus torques that are in opposite directions on 1 and 2. That is, for most positions of the pedal, τ_1 has the opposite sign of τ_2, and therefore, P_1 and P_2 have opposite signs while P_3 is smaller. This means that actuators on 1 and 2 must be large to handle significant torques at speeds around 1–2 Hz, but actuators on 3 and 4 can be significantly smaller.

Figure 13 compares the power requirements for two cycles of the device at 1-2 versus 3-4. (This power is required at either 1-2 or 3-4, but not both.) Here, positive power means energy flowing from actuator to device and user. First, note that the net power at each location is the same and always negative—the device is always receiving significant net power from the user. Second, note that the powers at 1 and 2 are nearly opposite and equal—this is as expected. Finally, note that the power required at 3 is always negative—the damper is always drawing power from the system. This was not enforced by the simulation; it is a result of choosing 3-4 over 1-2.

These plots show the benefit of applying actuators to 3 and 4 instead of 1 and 2. Figure 14 shows the powers on a speed-torque plot. Note that 1 and 2 require 1400 and 1650 W motors, but 3 and 4 only require 750 and 470 W actuators. Thus, the actuators needed are a 750 W damper on 3 and a 470 W motor on 4.

6.3 Passivity. The results from the simulation suggest that a purely passive device is feasible for lower-limb robots. Since the net energy flow is always from user to device, an ideal (friction-less) device would be able store that energy and return it when needed. This ideal device would use passive actuators, making it safer and nonenergy consuming. Furthermore, because the user is putting hundreds of watts into the device, it seems reasonable that even a nonideal (friction-containing) device would have enough net power input to overcome inefficiencies while still being passive.

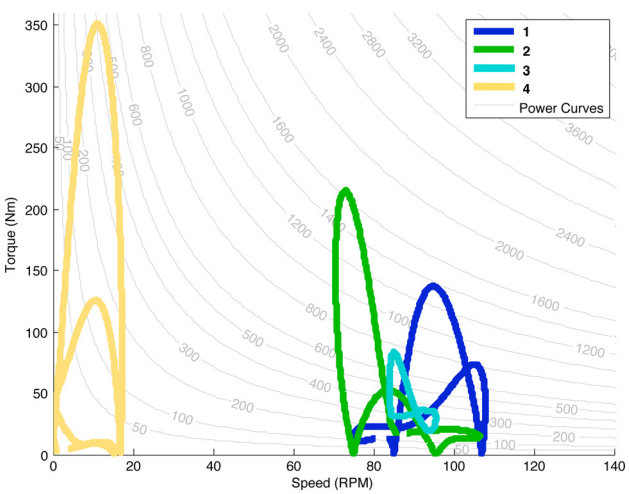

Fig. 14 Speed-torque curves for actuators on 1-2 versus 3-4

Downloaded 25 Aug 2011 to 141.209.167.245. Redistribution subject to ASME license or copyright; see http://www.asme.org/terms/Terms_Use.cfm

7 Conclusion

The design presented here is of a promising lower-limb exercise robot. The inertia, damping, and path actuation can be added to the system such that the path actuator does not feel the inertia or damping, or *vice versa*.

Going against conventional robotics wisdom, this device repeatedly, intentionally, and successfully travels through multiple singularities each cycle. The robot is well behaved because the inertia, path definition, and controller are all on the cyclic side of the singularities. In fact, the singularities help the controller because they reduce the user's influence on the actuators. Unfortunately, these singularities also restrict the set of possible pedal paths achievable by the device without further (offline) actuation.

Finally, an in-depth simulation of the design shows that the device will require reasonably sized motors and dampers. It suggests that, with further designing, the device could use purely passive actuators.

References

[1] DeJong, B. P., Colgate, J. E., and Peshkin, M. A., 2009, "Design of a Cyclic Robot for the Lower Limb," *ASME 2009 International Mechanical Engineering Congress and Exposition*, ASME, Orlando, FL, pp. 83–91.

[2] Duncan, P., Richards, L., Wallace, D., Stoker-Yates, J., Phol, P., Luchies, C., Ogle, A., and Studenski, S., 1998, "A Randomized, Controlled Pilot Study of a Home-Based Exercise Program for Individuals With Mild and Moderate Stroke," Stroke, **29**, pp. 2055–2060.

[3] Brown, D. A., and Kautz, S. A., 1998, "Increased Workload Enhances Force Output During Pedaling Exercise in Persons With Poststroke Hemiplegia," Stroke, **29**, pp. 598–606.

[4] Zeni, A. I., Hoffman, M. D., and Clifford, P. S., 1996, "Energy Expenditure With Indoor Exercise Machines," J. Am. Med. Assoc., **275**(18), pp. 1424–1427.

[5] Glass, S. C., and Chvala, A. M., 2001, "Preferred Exertion Across Three Common Modes of Exercise Training," J. Strength Cond. Res., **15**(4), pp. 474–479.

[6] DeJong, B. P., 2007, "On Cyclic Robots for the Lower Limb," Ph.D. thesis, Northwestern University, Evanston, IL.

[7] Shields, J., and Horowitz, R., 1998, "Adaptive Step Rate Control of a Stair Stepper Exercise Machine," Am. Control Conf., **2**, pp. 1058–1062.

[8] Ferber, A. R., 2007, "Affecting Exercise Intensity Through Haptic Communications," M.Sc. thesis, Northwestern University, Evanston, IL.

[9] Jezernik, S., Colombo, G., Keller, T., Frueh, H., and Morari, M., 2003, "Robotic Orthosis Lokomat: A Rehabilitation and Research Tool," Neuromodulation, **6**(12), pp. 108–115.

[10] Veneman, J., Kruidhof, R., Hekman, E., Ekkelenkamp, R., Asseldonk, E. V., and van der Kooij, H., 2007, "Design and Evaluation of the Lopes Exoskeleton Robot for Interactive Gait Rehabilitation," IEEE Trans. Neural Syst. Rehabil. Eng., **15**(3), pp. 379–386.

[11] Hesse, S., and Uhlenbrock, D., 2000, "A Mechanized Gait Trainer for Restoration of Gait," J. Rehabil. Res. Dev., **37**(6), pp. 701–708.

[12] Schmidt, H., Werner, C., Bernhardt, R., Hesse, S., and Kruger, J., 2007, "Gait Rehabilitation Machines Based on Programmable Footplates," J. Neuroeng. Rehabil., **4**(2), pp. 1–7 .

[13] Christensen, R. R., Hollerbach, J. M., Xu, Y., and Meek, S. G., 2000, "Inertial-Force Feedback for the Treadport Locomotion Interface," Presence, **9**(1), pp. 1–14.

[14] Boian, R. F., Bouzit, M., Burdea, G. C., Leswis, J., and Deutsch, J. E., 2005, "Dual Stewart Platform Mobility Simulator," *9th International Conference on Rehabilitation Robotics*, IEEE, Chicago, IL, pp. 550–555.

[15] Hollerbach, J., Grow, D., and Parker, C., 2005, "Developments in Locomotion Interfaces," *9th International Conference on Rehabilitation Robotics*, IEEE, Chicago, IL, pp. 522–525.

[16] Kazerooni, H., and Her, M. G., 1993. "A Virtual Exercise Machine," *IEEE International Conference on Robotics and Automation*, IEEE, Atlanta, GA, pp. 232–238.

[17] Public Health Service–U.S. Department of Health and Human Services, 1999, *Promoting Physical Activity: A Guide for Community Action*, Human Kinetics. Champaign, IL.

[18] Johnson, A. N., Cooper, D. F., and Edwards, R. H. T., 1977, "Exertion of Stair-climbing in Normal Subjects and in Patients With Chronic Obstructive Bronchitis," Thorax, **32**, pp. 711–716.

[19] Pearson, S. J., Cobbold, M., and Harridge, S. D. R., 2004, "Power Output of the Lower Limb During Variable Inertial Loading: A Comparison Between Methods Using Single and Repeated Contractions," Eur. J. Appl. Physiol. Occup. Physiol., **92**, pp. 176–181.

[20] Ulmer, H.-V., Janz, U., and Lollgen, H., 1977, "Aspects of the Validity of Borg's Scale. Is It Measuring Stress or Strain?," *Physical Work and Effort*, G. Borg, ed., Pergamon Press, New York, pp. 181–196.

[21] Fauling, E. L., Colgate, J. E., and Peshkin, M. A., 2004. "A High Performance 6-DOF Haptic Cobot," *IEEE International Conference on Robotics and Automation*, IEEE, New Orleans, LA, pp. 1980–1985.

[22] PheoniX Technologies Incorporated, 2007, www.ptiphoenix.com.

[23] Ivanenko, Y. P., Grasso, R., Macellari, V., and Lacquaniti, F., 2002, "Control of Foot Trajectory in Human Locomotion: Role of Ground Contact Forces in Simulated Reduced Gravity," J. Neurophysiol., **87**, pp. 3070–3089.

Downloaded 25 Aug 2011 to 141.209.167.245. Redistribution subject to ASME license or copyright; see http://www.asme.org/terms/Terms_Use.cfm